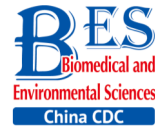# Letter to the Editor

A Functionalized Multi-walled Carbon Nanotube and Gold Nanoparticle Composite-modified Glassy Carbon Electrode for the Detection of Enterovirus 71[*]

CHENG Jing[1,2], KOU Jing[2], FAN Zhao Yu[2], HAN Yi Qun[2], MEI Yong[2],

GUO Zhen Zhong[2,#], and ZHAN Jian Bo[3,#]

Hand, foot, and mouth disease (HFMD) is a common infectious disease in children, occurring primarily in preschool children[1-3] with infants under three years old being generally susceptible. The disease is caused by various enteroviruses, among which EV71 and Coxsackievirus A group 16 (Cox A16) are the most common[4]. According to information released by the Chinese Center for Disease Control and Prevention on June 8, 2016, EV71 infection-related HFMD has been prevalent among infants and young children in China since 2007, with a high incidence and many deaths. About 13.8 million cases of HFMD were reported in China from 2008-2015, with an average incidence of 147/100,000; about 130,000 severe cases and more than 3,300 deaths were reported. Among HFMD cases with laboratory etiological diagnoses, positive rates of EV71, Cox A16, and other enteroviruses were 44%, 25%, and 31%, respectively. Among them, 74% of severe cases, 71% resulting in death, were EV71-positive. Overall, the positivity rate of EV71 in cases resulting in death was 93%. Given its higher mortality and severity rates compared to CoxA16 and other enteroviruses, EV71 has become a serious public health concern and has attracted a great deal of attention from the social and health sectors[5-7]. Children are the most susceptible to this disease and effective prevention and treatment measures are lacking, although an EV71 vaccine currently on the market has been shown to safely prevent and control the disease in China[8]. The development of a simple and rapid method for the early detection of EV71 is essential for early treatment of EV71 infections[1].

Biosensors are high-tech devices that integrate biology, chemistry, physics, medicine, and electronics technologies. Many such devices offer good selectivity, high sensitivity, fast analysis speeds, low cost, and continuous online monitoring in complex systems. Recent decades have seen the development of highly automated, miniaturized, and integrated features[2]. Biosensors have been accepted in a wide range of applications across a variety of fields including food safety, the pharmaceutical and chemical industries, clinical examination, biomedicine, and environmental monitoring. In particular, the combination of molecular biology with new technologies, such as microelectronics, optoelectronics, microfabrication, and nanotechnology, is changing the face of traditional medicine.

Common methods for detecting EV71 include virus isolation and culturing, serology, and RT-PCR methods. Viral culturing is relatively time-consuming and requires specialized technicians, and the sensitivity of serological methods is relatively low. Common RT-PCR detection is susceptible to contamination and provides only qualitative results. Although recent years have seen the development of quantitative PCR technologies that can accurately determine viral loads in unknown samples, and that can quickly detect c4 type EV71 virus[3], these technologies remain prohibitively expensive for widespread global applications.

This report describes the development of a sensitive, simple, rapid, and inexpensive biosensor for EV71 detection. The biosensor platform is based on carbon nanotubes (CNTs), which boast a high

specific surface area, excellent conductivity, and more chemical reaction sites than graphene. While the unique structure of CNTs results in several superior properties, the large number of π-bonds on their surface limits their dispersion in aqueous and organic solvents and severely limits their widespread application. Although some CNTs can be dispersed in certain solvents with the aid of ultrasonication, they usually precipitate immediately afterward. However, the solubility and dispersibility of CNTs can be enhanced by surface modification or functionalization. This study addressed the above problems by employing carboxylated multi-walled carbon nanotubes (MWCNTs) in the presence of chitosan as a solubility enhancer[4]. Chitosan (CHIT) is a natural biopolymer with high viscoelasticity, water permeability, and biocompatibility. It can be easily modified chemically and exhibits a good film-forming ability. Recent studies have shown that CNTs will more readily dissolve and diffuse throughout solvents in the presence of CHIT, thereby significantly broadening the application prospects of CNTs in chemical sensors and biosensor electrodes[5].

Although CNT-modified electrodes tend to respond to neurotransmitters and NADH, other biological substances do not elicit an electrochemical response. In order to broaden the analyte range of such electrodes, we combined CNTs with gold nanomaterials to create composite membrane-modified electrodes. Gold nanoparticles (AuNPs) are widely used as sensing materials because of their electron transfer ability, catalytic activity, sensitivity, and analyte selectivity. Single or multi-layer nano-gold films have a large specific surface area, which lends itself to good electrical conductivity and macroscopic tunneling, providing a means of signal amplification. Electrochemical biosensors have been fabricated based on the synergistic effects of CNTs and metal nanoparticles in terms of signal amplification[6]. AuNPs can be combined with amino-modified CNTs to form composite films with enhanced electrocatalytic properties.

This biosensor was established by a glassy carbon electrode with a combination of CHIT, functionalized MWCNTs (FCNTs), and AuNPs. Differential pulse voltammetric (DPV) experiments using these modified electrodes yielded significantly amplified signals. Bovine serum protein, which acts as a stabilizer against protein invariance, was used to obtain a stable biosensor with a high sensitivity for EV71. The peak current at the modified electrode decreased linearly with increasing EV71 titer. The developed biosensor also exhibited good selectivity for EV71 in the presence of interferents. Compared with other electrochemical biosensors, this biosensor has a great detection ability for EV71 (Table 1).

The innovation of this biosensor is that previous biosensors detect virus through the reaction of antigens and antibodies, while in this study, we directly detected virus strains and obtained accurate detection results and low detection limit for EV71.Compared with antigen detection, direct detection of virus strains is more consistent with the detection of clinical samples in real life. In addition, previous sensors could not well distinguish between EV71 and coxsackie A16, but this sensor could maintain a high selectivity specificity for EV71, while no specificity for coxsackie A16 , which proved that the sensor has a good selectivity.

EV71 virus (EU703812, $10^{8.75}$ $CCID_{50}$/mL) was acquired from the Hubei Provincial Center for Disease Control and Prevention. Anti-EV71 (1 mg/mL) was purchased from Abcam. Carboxylated MWCNTs (20 nm), chitosan (CHIT), glutaraldehyde (GTA), bovine serum albumin (BSA), tetrachloroauric acid trihydrate ($HAuCl_4 \cdot 3H_2O$), potassium ferricyanide {$K_3[Fe(CN)_6]$}, potassium ferrocyanide {$K_4[Fe(CN)_6]$}, sodium chloride (NaCl), potassium chloride (KCl), sodium dihydrogen phosphate (NaH_2PO_4), disodium hydrogen phosphate ($Na_2HPO_4 \cdot 12H_2O$) acetone, ethanol, and ether were purchased from Sigma-Aldrich. All reagents were used without further purification. Phosphate buffer solutions (PBS, 0.1 mol/L, pH 6.0) were prepared with Na_2HPO_4 and NaH_2PO_4 and the pH was adjusted with

Table 1. Comparison of EV71 Detection with Different Electrochemical Biosensors

Electrode	Trimming Material	Actual Samples	Range of linearity	LOD	Ref
ITO	AuNPs/DL-MBs/EV71mAb/HPR	Clinical EV71 samples	0-1,000 ng/mL	0.01 ng/mL	[9]
GCE	PoPD/AuNPs/EV71Ab/BSA	Environmental samples	0.1-80 ng/mL	0.04 ng/mL	[10]
GCE	CHIT-MWCNTs/AuNPs	Clinical serum sample	$10^{-4.25}$-$10^{0.75}$ $CCID_{50}$/mL	$10^{-4.72}$ $CCID_{50}$/mL	This work

0.1 mol/L NaOH and HCl. All other reagents were of analytical grade and aqueous solutions were prepared with double distilled water.

Electrochemical measurements were carried out on a CHI600E/700E Series Electrochemical Analyzer/Workstation (Chenhua Instruments, Shanghai, China) using a conventional three-electrode system comprised of a platinum foil counter electrode, a saturated calomel electrode (SCE) reference, and FCNTs-CHIT-AuNP-modified glassy carbon electrode (3 mm diameter) FCNTs-CHIT-AuNPs/GCE as the working electrode. The surface of the glassy carbon electrode was lightly ground with an Al_2O_3 powder, rinsed with distilled water and gently dried with nitrogen. The electrode was ultrasonically washed in ethanol and then in distilled water for 5 min each prior to use. Flakes of CHIT were dissolved in acetic acid (2.0 mol/L) to 0.50% w/v and stored at 4 °C. Then, 5.0 μL of 25% GTA were added to the CHIT solution (1.0 mL) as a cross-linking agent to form GTA/CHIT mixture solution. Then, 1.2 mg FCNTs were added into 1.0 mL of the mixture solution. The resulting material was mixed well in an ultrasonicated bath, yielding a uniform black suspension. Two microliters of the black suspension was dropped onto the surface of the glassy carbon electrode and irradiated with an infrared lamp for 10 min to dry. One milliliter of 1 wt% tetrachloroauric acid trihydrate solution was added to 100 mL of distilled water and kept at a boil. Rapidly, 1.5 mL of 1 wt% sodium citrate solution was added to the reaction mixture, which gradually turned red, indicating the formation of AuNPs (5 nm diameter). The solution was boiled for another 10 min, cooled to room temperature with constant stirring, and stored at 4 °C. To prepare AuNP-modified electrodes, 4.5 μL of the prepared AuNP solution was dropped onto the surface of the FCNTs-CHIT/GCE and dried under an infrared light for 10 min[7]. Ten microliters of anti-EV71 (20 ng/mL) solution (0.1 mol/L PBS, pH 7.4) was spread onto the modified GCE surface and stored at 4 °C for 12 h. The electrode was then washed with PBS (pH 6.0) and blown dry with a gentle stream of nitrogen. In order to block any remaining active sites and avoid nonspecific adsorption, the electrode was coated with a 10-μL drop of BSA solution (10 mg/mL) for 30 min at 37 °C. Finally, the modified electrode was washed with PBS (pH 6.0) and stored at 4 °C. Supplementary Figure S1 (available in www.besjournal.com) presents the design and fabrication of the FCNTs-CHIT/GCE/AuNP biosensor.

Prepared electrodes were characterized by cyclic voltammetry (CV) in a $Fe(CN)_6^{4-/3-}$ solution across a potential range of -0.20 V to +0.60 V (vs. SCE) at a scan rate of 100 mV/s for 10 cycles. Differential pulse voltammetry (DPV) was used to measure EV71 titer. For calibration, the original virus solution was diluted with D Hanks solution to a series of titers ranging from $10^{-4.25}$ $CCID_{50}$/mL to $10^{0.75}$ $CCID_{50}$/mL. For DPV measurements, 10 μL of EV71 solution, from low concentration to high concentration, were dropped onto the electrode surface and held for 60 min. EV71 was detected as a peak in the DPV voltammogram. The electrode was gently rinsed with PBS, dried with nitrogen, and sequentially washed with ethanol and distilled water in an ultrasonication bath between each sample.

Supplementary Figure S2 (available in www. besjournal.com) presents the step-by-step assembly of a prepared biosensor, characterized by CV in 0.1 mol/L PBS buffer at pH 6.0. A pair of well-defined redox peaks was observed on FCNTs-CHIT/GCE (curve a). This reversible one-electron redox peak was attributed to the $Fe(CN)_6^{4-}$ and $Fe(CN)_6^{3-}$ redox couple. The morphology and structure of carboxylated multi-walled carbon nanotubes treated with GTA and CHIT were determined by TEM. As shown in Figure 1, the TEM image shows a porous tubular structure of FWCNTs with a smooth surface and good dispersibility. They are mutual coupling between each other to form reticular structure, which further increased the specific surface area of the electrode and the effective binding area of the target, which indicate that it has good adsorption. After the immobilization of AuNPs onto the surface of
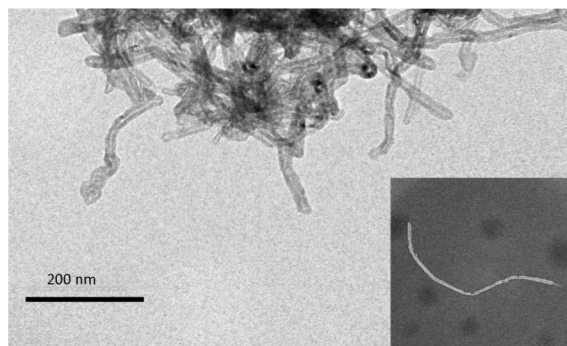

200 nm

Figure 1. The TEM image of MWNTs on the GCE. The lower right corner is a functionalized multi-walled carbon nanotube with smooth surface and tubular structure after dilution of 10 times.

the FCNTs-CHIT/GCE, the peak current corresponding to $Fe(CN)_6^{4-/3-}$ decreased (curve b). The reason for this decrease in current is the negative charge of the AuNPs, which effectively prevents the adsorption of $AuCl_4^-$ during the fabrication process and repels $Fe(CN)_6^{4-/3-}$ anions. The peak current decreased significantly with the fixation of anti-EV71 onto the immunosensor surface (curve c). A further decrease in current was observed after blocking the immunosensor with 10 mg/mL BSA (curve d). This response indicates that the attachment of BSA, a biological macromolecule, significantly restricted the access of $Fe(CN)_6^{4-/3-}$ to the immunosensor surface[7].

The pH of the PBS buffer significantly influenced the current response of our electrochemical immunosensor. The electrochemical behavior of the $Fe(CN)_6^{4-/3-}$ redox couple is affected by pH[11], and an unsuitable pH can result in protein denaturation. DPV was used to monitor the response of a FCNTs-CHIT-AuNPs-Anti-EV71-BSA/GCE sensor in a PBS solution containing $Fe(CN)_6^{4-/3-}$ from pH 5.0 to 7.5. As shown in Supplementary Figure S3A (available in www.besjournal.com), a peak current appeared near pH 6.0 with the position of the peak shifting slightly to the right with increasing pH. The absolute value of the peak current was largest at pH 6.0 and this value was chosen as optimal for all studies.

The condition used to immobilize FCNTs-CHIT on the surface of the GCE can also affect the electrochemical response of the biosensor. As shown in Figure S3B three reversible redox peaks with clear boundaries appeared, corresponding to a) infrared drying for 10 minutes, b) drying at room temperature for four hours, and c) blowing dry with a stream of nitrogen, respectively. Drying *via* infrared irradiation for 10 minutes yielded the highest redox currents and the most stable configuration at the electrode surface. Infrared drying acts through radiative heat transfer. Both moisture and heat diffuse through the material in the same direction, thereby accelerating drying. Infrared irradiation for 10 minutes was selected as the optimal drying method for FCNTs-CHIT/GCE fabrication. The effect of incubation conditions during AuNP immobilization on immunosensor behavior was also evaluated. The volume of AuNP solution during the immobilization reaction was varied from 3.0 μL to 10.0 μL (Figure S3C. Current response increased with increasing AuNP solution volume up to 4.5 μL, and then began to decline. Thus,

4.5 μL was adopted as the optimum volume of AuNP solution during immunosensor fabrication.

DPV is particularly well-suited for this application because the effective diffusion area decreases with the formation of immunocomplexes at the electrode surface. Supplementary Figure S4 (available in www.besjournal.com) shows that the absolute value of the peak current decreased gradually as the concentration of EV71 solution increased from $1.0 \times 10^{-4.25}$ $CCID_{50}$/mL to $1.0 \times 10^{0.75}$ $CCID_{50}$/mL. Immunocomplex formation at the electrode effectively hinders electron transfer. Figure 2 shows that a good linear relationship, with a correlation coefficient of 0.9913, was obtained between the current response of the developed immunosensor and the concentration of EV71 from $1.0 \times 10^{-4.25}$ $CCID_{50}$/mL to $1.0 \times 10^{0.75}$ $CCID_{50}$/mL. The line equation of the sensor response is represented as I0-IX (μA) = 62.726-10.478[–logC($CCID_{50}$/mL)], yielding a detection limit of $10^{-4.72}$ $CCID_{50}$/mL (signal-to-noise ratio of 3).

In the actual clinical testing, how to distinguish the target substance to be tested from other substances is an important issue. It is necessary to evaluate the selectivity and specificity of the biosensor. In this experiment, four other viruses with the same titer ($10^{-0.25}$ $CCID_{50}$/mL) as EV71's will act as interference to detect the selectivity and stability of the immunosensor. The four viruses are Coxsachie virus A16 (Cox A16), Norovirus (NV), Bunia virus (SFTSV), and Hantaan virus (HV). Each group was
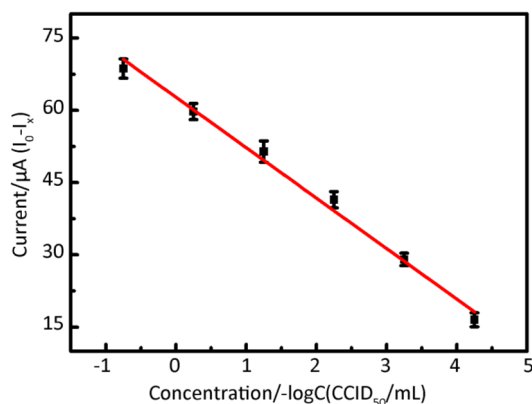

Figure 2. Calibration curve upon analysis of different concentrations of EV71 on the immunosensor, I_0-I_X(μA) = 62.726-10.478 [–logC ($CCID_{50}$/mL)](R^2 = 0.9913) (I_0: the peak current of the blank sample; I_X: the peak current of different concentrationsof EV71) (*n* = 3).

10 µL of EV71 plus 1 µL of interfering substance (except the first blank group). The exposure errors of all groups were all around 5%. And the Supplementary Figure S5 (available in www. besjournal.com) showed that the response signals of the 4 groups of interference did not change significantly, indicating that the sensor has good selectivity.

To demonstrate the potential of our as-prepared immunosensor for use in clinic applications, three healthy human serum specimens were obtained from the Hubei Provincial Center for Disease Control and Prevention and analyzed for EV71 using the proposed immunosensor. Supplementary Table S1 (available in www.besjournal.com) lists the results. Relative standard deviations were approximately 5%, indicating good analytical accuracy. Recoveries were calculated at 102.33%, 102.33%, and 91.21% respectively, indicating that the proposed method is a potentially reliable technique for determining human EV71 titer in real samples.

In addition, we also tested the repeatability and stability of the sensorit has been proved by many tests that the sensor has good repeatability, which can be used for 9 consecutive measurements effectively and accurately. Also, the established biosensor can be reused for 3 days under the condition of low temperature (4 °C) preservation. In order to verify this, we made intra and inter-day stability tests, relative standard deviation of the biosensor's detection results for EV71 are 0.41% and 1.63% (both are below 5%), which indicated its good stability. This report describes the development of a simple and effective method for immobilizing anti-EV71 antibody on a glassy carbon electrode via electrode modification with carboxylic MWCNTs. The resulting immunosensor was sensitive to the presence of EV71 virus in human serum. In the design process, GTA was used as a cross-linking agent to covalently bond anti-EV71 to the electrode. Chitosan provided a biocompatible microenvironment for anti-EV71 and allowed it to maintain its native biological activity. MWCNTs boast good electrical conductivity and are sensitive to changes in current generated by the reaction of antigens and antibodies. Our immunosensor boasts excellent sensitivity, high specificity, good reproducibility, and low cost. Additionally, experiments demonstrated that our sensor is suitable for use in applications requiring the detection of specific biological macromolecules, such as viruses. Of course, the sensor also has some limitations: for example, the time of sample pretreatment and electrochemical determination is too long to achieve real-time detection, at the same time, it has high requirements on the operating environment and can be greatly affected by the temperature. In the future, biosensors based on the platform described herein can be used to detect trace viruses in blood, urine, and other physiologi cal fluids, allowing for fast, simple, and accurate early diagnoses of various diseases.

#Correspondence should be addressed to ZHAN Jian Bo, Tel: 86-27-87650058, E-mail: jbzhan8866@163.com; GUO Zhen Zhong, Tel: 86-15071196433, E-mail: zhongbujueqi@ hotmail.com

Biographical note of the first author: CHENG Jing, female, born in 1984, PhD, majoring in biomedical analysis (Nutrition and chronic disease and related biomarker detection).

## REFERENCES

1. Chen H, Cheng Y, Liang X, et al. Molecular characterization of enterovirus 71 sibling strains for thermal adaption in Vero cells with adaptive laboratory evolution. Infect Genet Evol, 2019; 67, 44-50.
2. Han J, Ma XJ, Xu WB, et al. EV71 viral secretion by symptomatic hand foot and mouth disease patients and their asymptomatic close contacts. J infect, 2011; 62, 107-8.
3. Li HG, Lao Qun. The pulmonary complications associated with EV71-infected hand-foot-mouth disease. Radiol Infect Dis, 2017; 4, 137-42.
4. Yang L, Liu Y, Li S, et al. A novel inactivated enterovirus 71 vaccine can elicit cross-protective immunity against coxsackievirus A16 in mice. Vaccine, 2016; 34, 5938 -45.
5. Hong CH, Hsieh CF, Tseng CS, et al. A nanobiosensing method based on force measurement of antibody-antigen interaction for direct detection of enterovirus 71 by the chemically modified atomic force microscopic probe. Microb Pathog, 2017; 111, 292-7.
6. Cooper G, Mao Q, Crawt L, et al. Establishment of the 1st WHO International Standard for anti-EV71 serum (Human). Biologicals, 2018; 53, 39-50.
7. Prabowo BA, Wang RYL, Secario MK, et al. Rapid detection and quantification of Enterovirus 71 by a portable surface plasmon resonance biosensor. Biosens Bioelectron, 2017; 92, 186-91.
8. Narwal V, Deswal R, Batra B, et al. Cholesterol biosensors: A review. Steroids, 2019; 143, 6-17.
9. Kong Y, Li J, Wu S, et al. Functionalization of poly(o-phenylenediamine) with gold nanoparticles as a label-free immunoassay platform for the detection of human enterovirus 71. Sensors and Actuators B: Chemical, 2013; 183, 187-93.
10.Hou YH, Wang JJ, Jiang YZ, et al. A colorimetric and electrochemical immunosensor for point-of-care detection of enterovirus 71. Biosens Bioelectron, 2018; 99, 186-92.
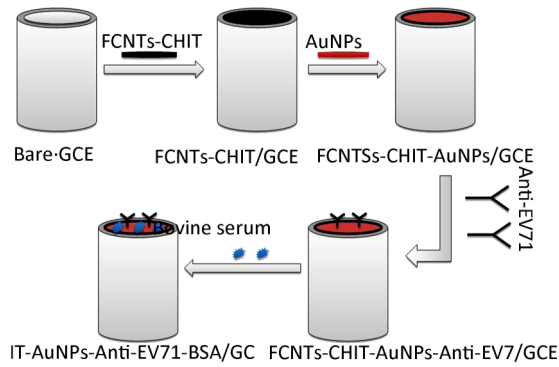
Supplementary Figure S1. Schematic illustration of the fabrication process of the immunosensor.
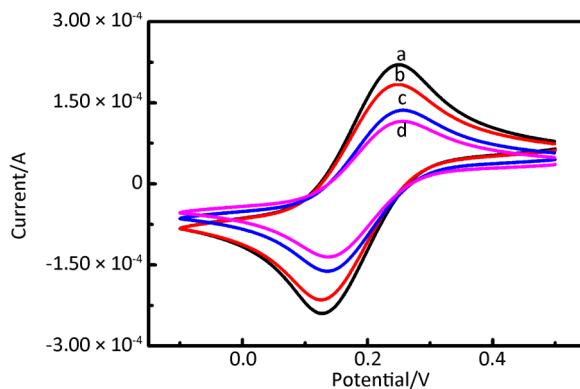

Supplementary Figure S2. Cyclic voltammograms recorded in 0.1 mol/L PBS containing $[Fe(CN)_6]^{4-/3-}$ with the scan rate of 100 mV/s after different steps of modification (n = 3): (a) FCNTs-CHIT/GCE, (b) AuNPs/FCNTs-CHIT/GCE, (c) AuNPs/FCNTs-CHIT-AntiEV71/GCE, and (d) AuNPs/FCNTs-CHIT-Anti-EV71-BSA/GCE.
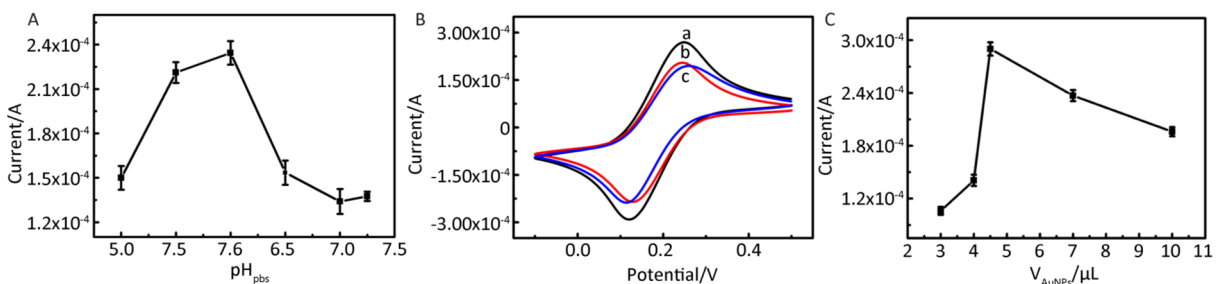
Supplementary Figure S3. Optimization of experimental parameters forelectrochemicalimmun. osensor: (A) PH of the PBS. Using AuNPs/FCNTs-CHIT-Anti-EV71-BSA/GCE, the peaks of DPVwererecorded in different pH of PBS (pH = 5.0-7.5) containing $Fe(CN)_6^{3-/4-}$, with the scan rate of 100 mV/s. (B) Different immobilization conditions of FCNTs-CHIT/GCE (a: Infrared drying for 10 minutes; b: Dry at room temperature for four hours; c: Nitrogen blow dry). CV scans of different conditions for AuNPs/FCNTs-CHIT-Anti-EV71-BSA/GCE, potential range is from -0.20 V to +0.60 V *vs.* SCE, the scan rate is 100 mV/s. (C) the quantity of AuNPs (n = 3). Using AuNPs /FCNTs-CHIT-Anti-EV71-BSA/GCE, the peaks of DPV were recorded in different quantity of AuNPs containing $Fe(CN)_6^{4-/3-}$, with the scan rate of 100 mV/s.
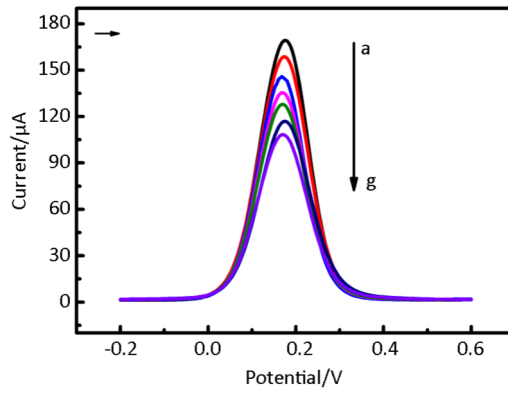
Supplementary Figure S4. DPV scans of different concentrations of EV71 for AuNPs/FCNTs-CH.IT-Anti-EV71-BSA/GCE, potential range is from -0.20 V to +0.60 V *vs.* SCE, the scan rate is 100 mV/s. From a to g, the EV71 concentration rang is from 0, $10^{-4.25}$, $10^{-3.25}$, $10^{-2.25}$, $10^{-1.25}$, $10^{-0.25}$, $10^{0.75}$.
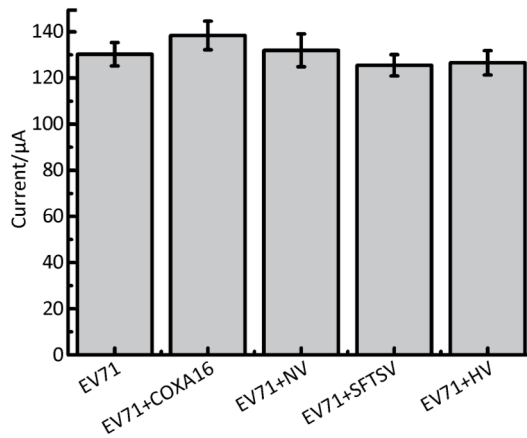
Supplementary Figure S5. The histogram in the figure shows that the current of different samples of EV71 interfered with by Cox A16, NV, SFTSV, and HV successively (n = 3).

Supplementary Table S1. Determination of Different Concentrations of EV71 in Serum Specimens

Sample	EV71 Found (CCID$_{50}$/mL)	EV71 Added (CCID$_{50}$/mL)	EV71 Detected (CCID$_{50}$/mL)	Recovery (%)	RSD (%)
Serum 1	0	$10^{-3.25}$	$10^{-3.24}$	102.33	4.55
Serum 2	0	$10^{-1.25}$	$10^{-1.24}$	102.33	5.28
Serum 3	0	$10^{0.75}$	$10^{0.71}$	91.21	5.24